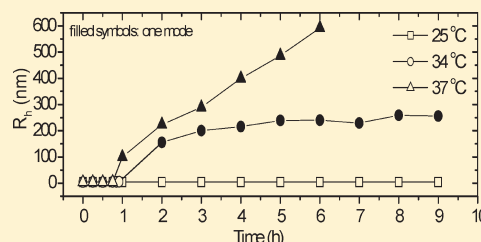


# Temperature-Induced Aggregation Kinetics in Aqueous Solutions of a Temperature-Sensitive Amphiphilic Block Copolymer

Atoosa Maleki,<sup>†,‡</sup> Anna-Lena Kjøniksen,<sup>†,‡</sup> Kaizheng Zhu,<sup>†</sup> and Bo Nyström<sup>\*,†</sup><sup>†</sup>Department of Chemistry, University of Oslo, P.O. Box 1033, Blindern, N-0315 Oslo, Norway<sup>‡</sup>Department of Pharmacy, School of Pharmacy, University of Oslo, Oslo, Norway

**ABSTRACT:** Time effects for the temperature-induced association complexes in solutions of the thermoresponsive poly(*N*-isopropylacrylamide)-*block*-poly(ethylene glycol)-*block*-poly(*N*-isopropylacrylamide) (PNIPAAm<sub>69</sub>-*b*-PEG<sub>23</sub>-*b*-PNIPAAm<sub>69</sub>) copolymer that exhibit a lower critical solution temperature were studied by means of turbidimetry and dynamic light scattering (DLS). The DLS results clearly show that at temperatures below the cloud point (CP) unimers coexist with intermicellar structures, which contract as the CP is approached. At this stage, no time effect was detected. At temperatures above the CP, large association structures are formed, and these aggregates dominate the decay of the correlation functions. A novel time-dependent growth of the aggregates was observed over several hours. The growth of the clusters is strengthened as the temperature rises, and this feature is supported by the turbidity results and the reduced scattered intensity experiments. For a low polymer concentration, an initial growth of the clusters is observed, whereas at longer times the apparent hydrodynamic radius from DLS is virtually constant. The results from this work stress the importance to check possible time effects in solutions of thermosensitive copolymers as the cloud point is approached.



## INTRODUCTION

The temperature-induced self-assembly of amphiphilic block copolymer chains in aqueous media and the observation of micelles and intermicellar structures are phenomena of interest not only because of their fundamental importance as related to polymer nanostructures<sup>1–4</sup> but also because of their various applications in nanotechnology, reusable elastomeric materials, electronics, and drug delivery.<sup>3,5,6</sup> In several investigations, the competition between temperature-induced interchain association and contraction has attracted a great deal of interest. In many studies on block copolymers, poly(*N*-isopropylacrylamide) (PNIPAAm) is employed as the thermoresponsive block, and the association and formation of intermicellar structures are frequently observed at elevated temperatures. PNIPAAm is a thermoresponsive water-soluble polymer that exhibits a lower critical solution temperature (LCST) at ca. 32 °C.<sup>7</sup> When the temperature is lower than the LCST, PNIPAAm is hydrophilic and can exist as individual chains with a random coil conformation in water, while, at higher temperatures, the PNIPAAm chain backbone becomes hydrophobic and collapses into individual single-chain globules or multichain aggregates, depending on the solution condition.<sup>8,9</sup> Studies on very dilute aqueous solutions of high molecular weight (the weight-average molar masses are typically larger than  $3 \times 10^6$  g/mol) PNIPAAm<sup>8,10,11</sup> and copolymers grafted with short polyethylene oxide chains<sup>2,12,13</sup> (PNIPAAm-*g*-PEO) have revealed a coil-to-globule transition upon heating the solutions. When a lower molecular weight sample (usually in the range  $3 \times 10^5$  to  $3 \times 10^6$  g/mol) is utilized, a higher polymer concentration is usually required to obtain reliable results. However, this concentration effect often leads to

an intricate interplay between coil-to-globule crossover and interchain aggregation at elevated temperatures.

The current understanding of self-assembly of amphiphilic copolymer chains into micelles and intermicellar complexes is mostly related to their equilibrium structures, whereas the kinetic aspects of the complex formation and the dynamics of the formed association structures have been far less investigated. The formation of aggregated nonequilibrium structures may constitute a severe complication in drug delivery applications. In some cases, time dependent association complexes are more decisive than equilibrium structures. For instance, complexes of oppositely charged components (e.g., polyelectrolytes and surfactants) are inclined to evolve highly aggregated nonequilibrium structures, whose formation can be either enhanced or repressed depending on the conditions of their formation.<sup>14</sup> Nonequilibrium structures can also be anticipated in aqueous solutions of PNIPAAm-based copolymers at elevated temperatures because of augmented hydrophobicity of the PNIPAAm block and higher sticking probability of the species. Very limited information is available on the growth kinetics of these aggregates and their dynamics. These issues are of crucial importance to our understanding of, and hence our ability to tailor, both the self-assembly process of core-shell nanoparticles and how to ultimately optimize their efficacy and stability.

In the past, various types of time-dependent phenomena in PNIPAAm systems have been reported.<sup>15–20</sup> Water uptake and

Received: March 19, 2011

Revised: June 23, 2011

Published: June 23, 2011

swelling kinetics of thermoresponsive thin films containing PNIPAAm have attracted a great deal of interest.<sup>18–20</sup> Time-resolved small-angle X-ray scattering measurements of spinodal decomposition in a chemically cross-linked NIPAAm gel were reported,<sup>15</sup> and the earliest steps in the volume collapse transition on length scales comparable to the average distance between cross-links and the correlation length of the gel were examined. For early times, the linear Cahn–Hilliard–Cook theory could be used to describe the time evolution of the scattered intensity. There are studies in the literature<sup>16,17</sup> addressing time effects in dilute solutions of PNIPAAm. Kajawa et al.<sup>16</sup> studied the kinetics of merging and/or chain exchange between mesoglobules formed in dilute aqueous solutions of fluorescently labeled PNIPAAm heated above their demixing temperature by utilizing fluorescence spectroscopy. In another study,<sup>17</sup> temperature-induced association of cyclic and linear PNIPAAm chains in dilute solutions was monitored by laser light scattering and stopped-flow temperature jump. It was argued that the temperature-jump-induced association of cyclic PNIPAAm chains in the stop-flow measurement revealed two kinetic growth stages, which were ascribed to the loose packing of contracted chains and further contraction-induced fragmentation of initially packed cyclic PNIPAAm chains as a result of a lack of entanglements. On the other hand, for linear PNIPAAm chains, the intrachain compression and interchain penetration/entanglement were reported to occur simultaneously with increasing temperature, leading to larger and more compact aggregates whose size increases with rising temperature.

In the present work, we have synthesized a triblock copolymer with two PNIPAAm blocks of the same length that are separated by a short hydrophilic poly(ethylene glycol) (PEG) spacer. The composition of the copolymer is PNIPAAm<sub>69</sub>-*b*-PEG<sub>23</sub>-*b*-PNIPAAm<sub>69</sub>. The chemical structure of the copolymer, together with an illustration of the molecular weight distribution determined by asymmetric flow field-flow fractionation (AF4) methods, is depicted in parts a and b of Figure 1. Depending on concentration and temperature, the unimers of this copolymer are foreseen to self-assemble into micelles and intermicellar structures in aqueous media. The fairly long PNIPAAm sequences at both ends should facilitate the formation of association complexes of this copolymer at elevated temperatures. The turbidity and dynamic light scattering results will demonstrate the growth of aggregates over a long time at fixed temperatures above the LCST. The experiments are carried out on 1 wt % solutions; this concentration is well below the overlap concentration to the semidilute concentration regime for this low molecular weight ( $M_w = 19\,100$ ) sample. At this concentration, both unimers and larger association complexes can be monitored at low temperatures. In addition, some turbidity and DLS measurements were also conducted at 0.2 wt %.

## EXPERIMENTAL SECTION

**Materials and Copolymer Synthesis.** The ABA triblock copolymer was prepared via a simple atom transfer radical polymerization (ATRP) procedure performed in aqueous media at ambient temperature.<sup>21,22</sup> Briefly, the polymerization was performed in a water/DMF (50:50, v/v) mixture solvent at 25 °C for 35 min, and the initiator/catalyst system in the mixture contained PEG-bis-functional macroinitiator (PEG-bis-MI), CuCl, and Me<sub>6</sub>TREN (with molar feed ratio [NIPAAm] = 2 M; [NIPAAm]/[PEG-bis-MI]/[CuCl]/[Me<sub>6</sub>TREN] = 140/1/2/2). The preparation

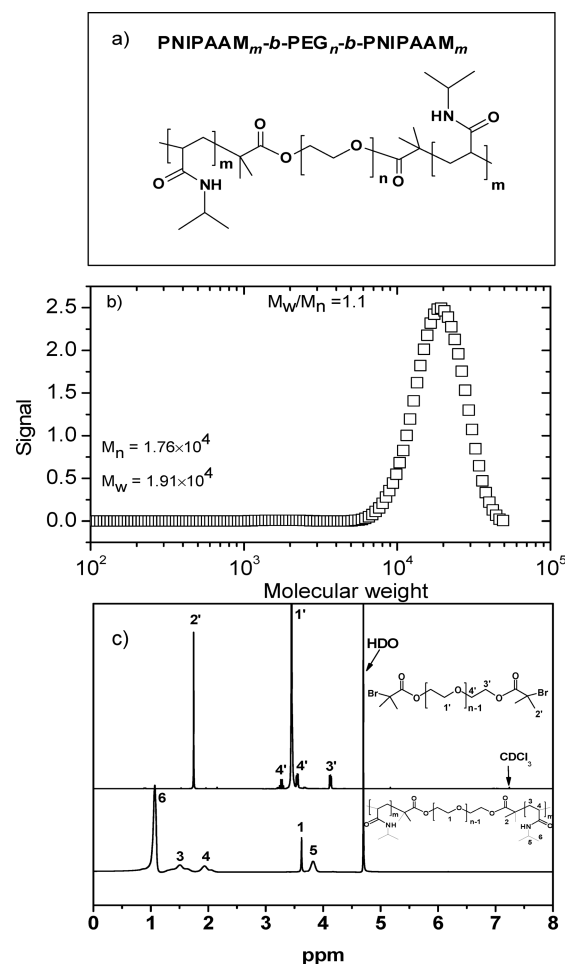


**Figure 1.** (a) Chemical structure of the thermoresponsive PNIPAAm<sub>m</sub>-*b*-PEG<sub>n</sub>-*b*-PNIPAAm<sub>m</sub> triblock copolymer, with values of *m* and *n* equal to 69 and 23, respectively. (b) Illustration of the molecular weight distribution of the triblock copolymer in aqueous solution (0.01 M NaCl), with the aid of AF4.  $M_n$ ,  $M_w$ , and the polydispersity index values are also given. (c) Chemical structure and NMR spectra (300 MHz, 25 °C) of the PEG<sub>1000</sub>-bis-MI (above, in CDCl<sub>3</sub>) and triblock copolymer (below, in D<sub>2</sub>O).

and purification procedures of the PEG-bis-MI and the polymer were conducted under similar conditions as described in detail previously.<sup>23,24</sup>

The chemical structure and composition of the PEG bis-functional macroinitiator (Br-PEG1000-Br) and the triblock copolymer were ascertained by their <sup>1</sup>H NMR spectra (Figure 1c). The number of repeating units of the ethylene glycol (EG) in the PEG polymer was recalculated according to its proton NMR spectrum of the fully esterification product on the basis of a simple formula:  $n = (3I_a/I_b)$ , where  $I_a$  is the corresponding integral area of the methylene group of EG (–O–CH<sub>2</sub>CH<sub>2</sub>–, 1', 3', and 4' in Figure 1) at about 3.7 ppm and  $I_b$  is the integral area of the end-capped methyl group (–C(CH<sub>3</sub>)<sub>2</sub>Br, 2' in Figure 1c) at 1.8 ppm. The number of repeating units of EG is estimated to be 23 for PEG<sub>1000</sub>, and it is denoted as PEG<sub>23</sub>. The unit numbers of the NIPAAm in P(NIPAAm)<sub>m</sub>-*b*-PEG<sub>n</sub>-*b*-P(NIPAAm)<sub>m</sub> were evaluated by comparing the integral areas of the methenyl proton peak (1) of EG (δ = 3.7 ppm) and the methylene proton peak (5) of PNIPAAm (δ = 3.85 ppm). The entire repeating units of

NIPAAM/PEG (2*m*/*n*) are estimated to be 138/23 on the basis of the previous calculation result that the number of EG units of PEG-bis-MI is 23. Therefore, the composition of the synthesized triblock copolymer is estimated to be *m*/*n*/*m* = 69/23/69 for P(NIPAAM)<sub>69</sub>-*b*-PEG<sub>23</sub>-*b*-P(NIPAAM)<sub>69</sub>.

**Asymmetric Flow Field-Flow Fractionation.** The asymmetric flow field-flow fractionation (AFFFF) measurements<sup>23</sup> were carried out on an AF2000 FOCUS system (Postnova Analytics, Landsberg, Germany) equipped with an RI detector (PN3140, Postnova) and a multiangle (seven detectors in the range 35–145°) light scattering detector (PN3070,  $\lambda$  = 635 nm, Postnova). The sample (1.0 wt % in 0.01 M NaCl) was measured using a 350  $\mu$ m spacer, a regenerated cellulose membrane with a cutoff of 1000 (Z-MEM-AQU-425N, Postnova), and an injection volume of 20  $\mu$ L. In the experiments, a constant detector flow rate of 1.0 mL/min was used. The focusing time was 6 min at a cross-flow of 2 mL/min. The cross-flow was then linearly reduced to zero during a period of time of 10 min. Processing of the measured data was achieved by the Postnova software (AF2000 Control, version 1.1.011). The molecular weight of the sample was determined using this software with a Zimm-type fit. The molecular weight and polydispersity of the sample are given in Figure 1b.

**Turbidity.** The turbidity measurements were conducted on an NK60-CPA cloud point analyzer (Phase Technology, Richmond, B.C., Canada). A detailed description of the equipment and determination of the turbidities has been given elsewhere.<sup>25</sup> This apparatus utilizes a scanning diffusive technique to characterize the phase changes of the sample with high sensitivity and accuracy. The light beam from an AlGaAs light source, operating at 654 nm, was focused on the measuring sample that was applied onto a specially designed glass plate that was coated with a thin metallic layer of very high reflectivity (mirror). Directly above the sample, an optical system with a light-scattering detector continuously monitored the scattered intensity signal (*S*) of the sample as it was subjected to prescribed temperature alterations. The relationship between the signal and the turbidity ( $\tau$ ) is given by the following empirical relationship:  $\tau$  (cm<sup>-1</sup>) = (9.0  $\times$  10<sup>-9</sup>)*S*<sup>3.751</sup>.<sup>25</sup>

**Dynamic Light Scattering.** The dynamic light scattering (DLS) experiments were conducted with the aid of an ALV/CGS-8F multidetector version compact goniometer system, with eight fiber-optical detection units (ALV-GmbH, Langen, Germany). The beam from a Uniphase cylindrical 22 mW HeNe-laser, operating at a wavelength of 632.8 nm with vertically polarized light, was focused on the sample cell (10-mm NMR tubes, Wilmad Glass Co., of highest quality) through a temperature-controlled cylindrical quartz container (with two plane-parallel windows and with the temperature constancy being controlled to within  $\pm 0.01$  °C with a heating/cooling circulator), which is filled with a refractive index matching liquid (*cis*-decalin). The polymer solutions were filtered in an atmosphere of filtered air through a 5  $\mu$ m filter (Millipore) directly into precleaned NMR tubes. The correlation function data were recorded continuously, with an accumulation time of 1 min at eight scattering angles simultaneously, in the angular range 22–141°.

## RESULTS AND DISCUSSION

In the past, little attention has been paid to the effect of time evolution of the association complexes and aggregation kinetics.<sup>16,17</sup> Generally, it is assumed that a steady state condition or equilibrium

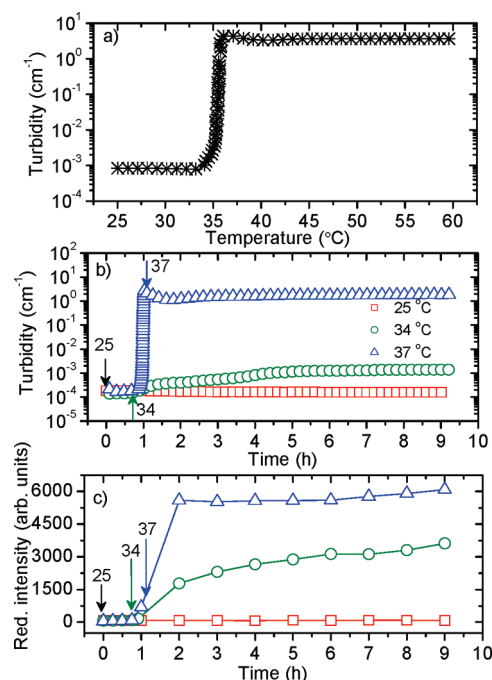


**Figure 2.** Turbidity and reduced scattered intensity measurements on 1 wt % aqueous solutions of the triblock copolymer. (a) Temperature dependence of the turbidity during heating at a rate of 0.2 °C/min. (b) Heating (0.2 °C/min) of the sample to the indicated temperatures and observation of the time evolution of the turbidity at this temperature. (c) The same procedure as in part b for the reduced scattered intensity. The arrows show the times when the indicated temperatures are reached.

is reached shortly after a temperature alteration. However, the present study clearly demonstrates that the growth of association complexes can continue for several hours at fixed temperatures above the cloud point.

The temperature-induced formation of micelles and intermolecular structures in aqueous solutions of amphiphilic copolymers has attracted a great deal of interest.<sup>23,26</sup> However, in most studies, equilibrium conditions were assumed in the analysis of the results from temperature-induced association complexes. There is lack of investigations addressing the kinetics of the growth of the clusters. This nonequilibrium state is a condition that may appear in solutions of amphiphilic copolymer species close to or above the cloud point of the PNIPAAM, where the entities become sticky and aggregation may occur over an extended period of time. The aim of this study is to probe the time evolution of the growth of these nonequilibrium structures and to establish the importance of this feature for thermoresponsive systems. For this purpose, we have carried out turbidity and dynamic light scattering (DLS) experiments on solutions of this triblock copolymer at fixed temperatures both below and above the cloud point.

The time effects are expected to be important at temperatures above the cloud point (CP). The effect of temperature on the turbidity is depicted in Figure 2a; the temperature at which the first deviation of the scattered intensity from the baseline occurred was taken as the cloud point, and the value of the CP was found to be 33 °C. The heating rate is 0.2 °C/min, and the transition is sharp with high values of turbidity. This shows that large association complexes are formed above the cloud point.



To probe the effect of time, the sample was heated ( $0.2\text{ }^{\circ}\text{C}/\text{min}$ ) from  $25\text{ }^{\circ}\text{C}$  to a preset temperature, and the time evolution of the turbidity was monitored over several hours (Figure 2b) at the preset fixed temperature. It takes about 40 min to heat the sample from  $25\text{ }^{\circ}\text{C}$  to the cloud point. At a constant temperature ( $25\text{ }^{\circ}\text{C}$ ) well below the CP, no time effect of the turbidity is observed. At  $34\text{ }^{\circ}\text{C}$  (slightly above the CP), a moderate increase in the turbidity occurs (low turbidity values) over 4–5 h before the turbidity flattens out. At  $37\text{ }^{\circ}\text{C}$  (far above the CP), the turbidity exhibits a sharp transition with high turbidity values, suggesting the formation of fast growing clusters. These turbidity features parallel the behaviors of the reduced scattered intensity obtained from DLS (Figure 2c). The results indicate that, at temperatures close to the CP, a moderate growth of interchain structures takes place, and it continues over several hours, while at temperatures well above the CP, large clusters are formed rapidly. This can be rationalized in the following way: as the temperature rises above the CP, the PNIPAAm moieties become gradually more hydrophobic, and this results in a higher sticking probability, which facilitates a faster growth of interchain structures because of a more efficient cluster formation when the species collide.

At temperatures below the CP, the dynamic light scattering (DLS) results reveal the existence of a fast (single exponential) and a slow (stretched exponential) relaxation mode, both of which are diffusive. For these dilute solutions, the scattered field obeys Gaussian statistics and the measured correlation functions  $g^2(q, t)$ , where the wave vector  $q = (4\pi n/\lambda) \sin(\theta/2)$ , with  $\lambda$ ,  $\theta$ , and  $n$  being the wavelength of the incident light in a vacuum, scattering angle, and refractive index of the medium, respectively, can be related to the theoretically amenable first-order field correlation function  $g^1(q, t)$  by the Siegert relationship<sup>27</sup>  $g^2(q, t) = 1 + B|g^1(q, t)|^2$ , where  $B$  is usually treated as an empirical factor. Under conditions below the CP, the correlation functions can be described by the sum of a single exponential and a stretched exponential function as follows:

$$g^1(t) = A_f \exp[-(t/\tau_f)] + A_s \exp[-(t/\tau_{se})^\beta] \quad (1)$$

with  $A_f + A_s = 1$ . The parameters  $A_f$  and  $A_s$  are the amplitudes for the fast and the slow relaxation modes, respectively. The stretched exponent  $\beta$  characterizes the width of the distribution of relaxation times. The variables  $\tau_f$  and  $\tau_{se}$  are the relaxation times characterizing the fast and the slow processes, respectively. Bimodal relaxation processes have been reported<sup>25,28,29</sup> from DLS studies on associating polymer systems of various natures. In the analysis of the correlation functions with the aid of eq 1, a nonlinear fitting algorithm was employed to obtain best-fit values of the variables  $A_f$ ,  $\tau_f$ ,  $\tau_{se}$ , and  $\beta$  appearing on the right-hand side of eq 1. The fast relaxation time yields the mutual diffusion coefficient  $D$  ( $\tau_f^{-1} = Dq^2$ ) of unimers, and  $\tau_{se}$  characterizes the dynamics of large clusters or intermicellar structures. Through the stretched exponent ( $0 < \beta \leq 1$ ), the mean relaxation time for the slow mode is given by the following equation:

$$\tau_s = \frac{\tau_{se}}{\beta} \Gamma\left(\frac{1}{\beta}\right) \quad (1a)$$

where  $\Gamma$  is the gamma function. From the relaxation modes, we are able to calculate the apparent hydrodynamic radii ( $R_{h,f}$  and  $R_{h,s}$ ) from the fast and slow relaxation times, respectively, via the Stokes–Einstein relationship  $R_h = k_B T / 6\pi\eta_0 D$ , where  $k_B$  is the Boltzmann constant,  $T$  is the temperature,  $\eta_0$  is the solvent

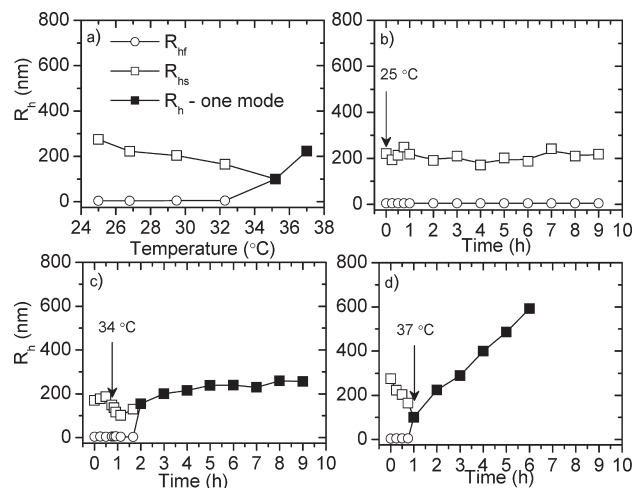


**Figure 3.** Dynamic light scattering measurements on 1 wt % aqueous solutions of the triblock copolymer. (a) Temperature dependences of the apparent hydrodynamic radii during heating at a rate of  $0.2\text{ }^{\circ}\text{C}/\text{min}$  from 25 to  $37\text{ }^{\circ}\text{C}$ . (b–d) Heating ( $0.2\text{ }^{\circ}\text{C}/\text{min}$ ) of the sample to the indicated temperatures and observation of the time evolution of the apparent hydrodynamic radii at this temperature. The arrows show the times when the indicated temperatures are reached. The filled symbols indicate the appearance of a single relaxation mode.

viscosity, and  $D$  is the diffusion coefficient of unimers or micelles/intermicellar complexes. The fast mode portrays the diffusion of single-chain molecules (unimers) with a hydrodynamic radius ( $R_{h,f}$ ) of about 4 nm, and the slow relaxation mode describes the diffusion of micelles or intermicellar structures with much larger hydrodynamic radii ( $R_{h,s}$ ).

At temperatures above the CP, the decays of the correlation functions are well portrayed by the following single stretched exponential function:

$$g^1(t) = \exp[-(t/\tau_{se})^\beta] \quad (2)$$

In this case, we have large clusters with a certain size distribution, and these species dominate the decay of the correlation function.

Figure 3a shows the hydrodynamic radii when a 1 wt % solution of the copolymer is continuously heated ( $0.2\text{ }^{\circ}\text{C}/\text{min}$ ) to  $37\text{ }^{\circ}\text{C}$ , which is well above the cloud point ( $33\text{ }^{\circ}\text{C}$ ). It is evident that up to the CP association complexes coexist with unimers and that at higher temperatures the population of large species dominates, and this leads to a single relaxation mode that yields high values of the hydrodynamic radius as the temperature rises far beyond the CP. In the temperature region below the CP, the large species contract with increasing temperature. This may be rationalized in the following way: the number of isopropyl side groups carried by the PNIPAAm complexes confers the hydrophobic character of the species, whereas the hydrophilic nature of the polymer is generated through the hydrogen bonding of water with the amide groups. At elevated temperatures, the hydrogen bonding with water is progressively disrupted on heating, and the hydrophobicity of the copolymer is enhanced with the packing of the hydrophobic segments, leading to temperature-induced compression of the species prior to interchain aggregation.<sup>9,13,25</sup>

The triblock copolymer sample (1 wt % concentration) in Figure 3b–d was heated to the preset temperature; thereafter, the temperature was kept constant, and the correlation functions were recorded continuously during several hours to depict the

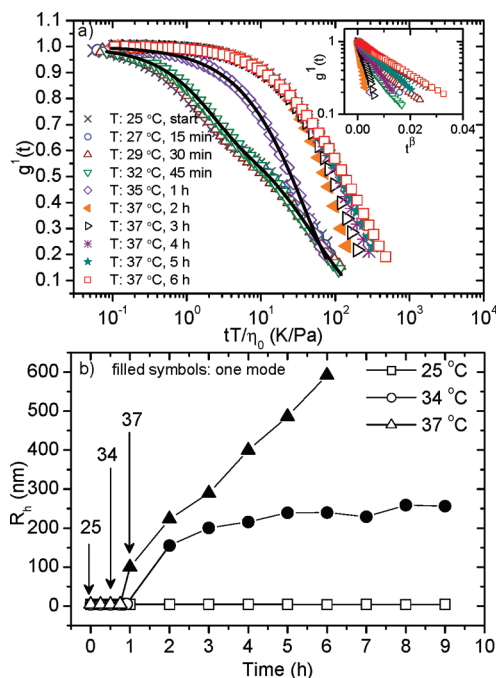


**Figure 4.** (a) First-order field correlation function (at a scattering angle of  $90^\circ$ ) versus the quantity  $tT/\eta_0$  for 1 wt % solutions of the triblock copolymer at the various temperatures and times indicated. Every second point is shown. The lines are fitted with the aid of eq 1 (two relaxation modes) or eq 2 (one relaxation mode). See the text for details. The inset plot demonstrates the stretched exponential character of the correlation function at long time. (b) Hydrodynamic radii as a function of time for 1 wt % polymer solution at the indicated fixed temperatures. The arrows show the times when the indicated temperatures are reached.

time evolution of the hydrodynamic radii. At 25 °C, no time dependence of  $R_{h,f}$  or  $R_{h,s}$  can be detected. During the heating process (0.2 °C/min) to 34 °C (above the CP), two relaxation modes are found, but in the course of the time evolution at this temperature, the profile of the correlation function is changed, and only one mode can be traced. It is evident that the species continue to grow over several hours. At the highest temperature (37 °C), two relaxation modes are again observed during the heating to the preset temperature, but a single mode evolves in the course of time at this temperature, and a strong increase of the hydrodynamic radius is registered over 5 h at this temperature.

In Figure 4, normalized time correlation function data at a scattering angle of  $90^\circ$  for 1 wt % solutions of the triblock copolymer at various temperatures and times are depicted in the form of semilogarithmic plots. The solid lines were fitted with the aid of eq 1 (two relaxation modes) for temperatures up to the CP, whereas at higher temperatures, the correlation functions were fitted with a single stretched exponential (eq 2). The correlation functions are well described by these expressions. The inset plot in Figure 4a shows a semilogarithmic plot of  $g^1(t)$  as a function of  $t^\beta$ . This type of plot yields straight lines for functions that can be represented by stretched exponentials. It is observed that the long time behaviors of the correlation functions are well described by straight lines. To take into account trivial changes of the solvent viscosity with temperature, the correlation data have been plotted against the quantity  $tT/\eta_0$ . At temperatures up to 32 °C, the correlation functions virtually collapse onto each

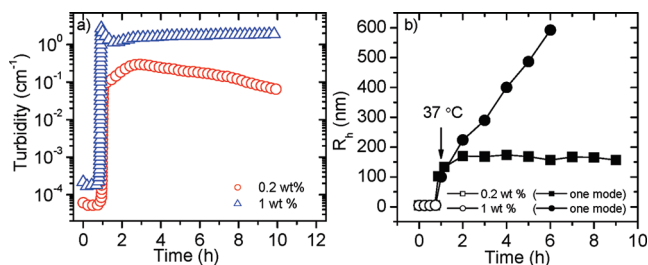


**Figure 5.** Comparison of turbidity and DLS results for two polymer concentrations (0.2 and 1 wt %) at 37 °C. Heating (0.2 °C/min) of the sample from 25 °C to the indicated temperature and observation of the time evolution of the turbidity (a) and the apparent hydrodynamic radii (b) at this temperature. The arrow shows the time when the indicated temperature is reached.

other, and the decay exhibits a bimodal character that can be portrayed by eq 1. At higher temperatures, the tails of the correlation functions are shifted toward longer times with increasing temperature and time evolution; the profile of the correlation functions is described by a single stretched exponential (eq 2). This may be rationalized in the way that, at low temperatures, unimers and micelles/intermicellar complexes coexist and give rise to the two modes, whereas, at temperatures above the CP, the large association complexes dominate the relaxation process.

A comparison of the time evolution of  $R_h$  at different temperatures is displayed in Figure 4b for a 1 wt % concentration of the copolymer. The results reveal that no time effects are detected at temperatures below the CP, but above the CP, the species grow in the course of time. This trend is strengthened as the temperature rises. The picture that emerges is that we have stabilized structures that are not affected by time below the CP, whereas, at temperatures above the CP, the stickiness of the species increases with the distance from the CP, and this results in the formation of large association complexes at long times.

To investigate the effect of polymer concentration on temperature-induced interchain aggregation, the time evolution of the turbidity and the apparent hydrodynamic radii for two different concentrations (0.2 and 1 wt %) at a preset temperature of 37 °C is depicted in Figure 5. Over the course of time, the turbidity exhibits sharp transitions for both concentrations at intermediate times, and at longer times the turbidity almost levels out with lower values for the low concentration sample. The DLS results reveal that  $R_h$  increases monotonously with time for the highest concentration, whereas  $R_h$  flattens out at times above 2 h for the low concentration sample and assumes a value of approximately 150 nm. This finding suggests that more chains can aggregate together at a higher polymer concentration. This may indicate that, at a low polymer concentration, a steady state condition emerges where the compact species are stabilized, whereas the loose structures formed at the higher concentration can more easily undergo interchain association/entanglement to form large aggregates. In dilute aqueous solutions of PNIPAAm,<sup>16</sup> it was found that the size of species depends on solution concentration. In a study<sup>17</sup> on cyclic and linear PNIPAAm in dilute solution, it was shown that the linear analogue can form interchain association at elevated temperatures, whereas the cyclic PNIPAAm forms stable mesoglobules at high temperatures.

## CONCLUSIONS

This work on solutions of a thermoresponsive triblock PNIPAAm based copolymer with a lower critical solution temperature has clearly demonstrated that, at temperatures below the cloud point, unimers coexist with intermicellar structures, which contract as the cloud point is approached. At this stage, no time effect is detected, and the turbidity and sizes of the species are constant in the course of time. At temperatures above CP, large association complexes (micelles and intermicellar structures) are formed, and these species dominate the decay of the correlation functions. A novel time-dependent growth of the aggregates is observed over several hours. The growth of the clusters is augmented by high temperature, and this feature is supported by the turbidity measurements and the reduced scattered intensity experiments. At a low polymer concentration (0.2 wt %), an initial growth of the species is observed, but at longer times, the size of the complexes is virtually constant. Previous studies<sup>8,9</sup> on contraction and association behavior in dilute aqueous solutions of PNIPAAm have shown that interchain aggregation depends on temperature and solution concentration, but the cluster growth over long times has not been examined.

This study stresses the importance of checking possible time effects in solutions of thermosensitive polymers as the cloud point is passed. The time effect can be vital in polymer systems containing PNIPAAm. There are a huge number of papers in the literature where copolymers containing PNIPAAm have been used, and this work emphasizes the importance of checking possible time-effects at temperatures close to or above the cloud point for temperature responsive polymers.

## AUTHOR INFORMATION

### Corresponding Author

\*E-mail: bo.nystrom@kjemi.uio.no.

## ACKNOWLEDGMENT

We gratefully acknowledge support from the Norwegian Research Council for Projects 177665/V30 and 177556/V30.

## REFERENCES

- (1) Muthukumar, M.; Ober, C. K.; Thomas, E. L. *Science* **1997**, *277*, 1225.
- (2) Qiu, X.; Wu, C. *Macromolecules* **1997**, *30*, 7921.
- (3) *Block Copolymers in Nanoscience*; Lazzari, M., Liu, G., Lecommandoux, S., Eds.; Wiley-VCH: Weinheim, Germany, 2006.
- (4) Förster, S.; Antonietti, M. *Adv. Mater.* **1998**, *10*, 195.
- (5) *Responsive Polymer Materials: Design and Applications*; Minko, S., Ed.; Blackwell Publishing: Ames, IA, 2006.
- (6) Malmsten, M. *Surfactants and Polymers in Drug Delivery*; Marcel Dekker: New York, 2002.
- (7) Schild, H. K. *Prog. Polym. Sci.* **1992**, *17*, 163.
- (8) Wu, C.; Wang, X. *Phys. Rev. Lett.* **1998**, *80*, 4092.
- (9) Lessard, D. G.; Ousaleh, M.; Zhu, X. X.; Eisenberg, A.; Carreau, P. J. *J. Polym. Sci., Part B: Polym. Phys.* **2003**, *41*, 1627.
- (10) Wu, C.; Zhou, S. *Macromolecules* **1995**, *28*, 5388.
- (11) Wang, X.; Qiu, X.; Wu, C. *Macromolecules* **1998**, *31*, 2972.
- (12) Chen, H.; Li, J.; Ding, Y.; Zhang, G.; Zhang, Q.; Wu, C. *Macromolecules* **2005**, *38*, 4403.
- (13) Chen, H.; Zhang, Q.; Li, J.; Ding, Y.; Zhang, G.; Wu, C. *Macromolecules* **2005**, *38*, 8045.
- (14) Mezei, A.; Mészáros, R.; Varga, I.; Gilányi, T. *Langmuir* **2007**, *23*, 4237.

- (15) Liao, G.; Xie, Y.; Ludwig, K. F., Jr.; Bansil, R.; Gallagher, P. *Phys. Rev. E: Stat. Phys., Plasmas, Fluids, Relat. Interdiscip. Top.* **1999**, *60*, 4473.
- (16) Kujawa, P.; Aseyev, V.; Tenhu, H.; Winnik, F. M. *Macromolecules* **2006**, *39*, 7686.
- (17) Ye, J.; Xu, J.; Hu, J.; Wang, X.; Zhang, G.; Liu, S. *Macromolecules* **2008**, *41*, 4416.
- (18) Wang, W.; Metwalli, E.; Perlich, J.; Troll, K.; Papadakis, C. M.; Cubitt, R.; Müller-Buschbaum, P. *Macromol. Rapid Commun.* **2009**, *30*, 114.
- (19) Wang, W.; Metwalli, E.; Perlich, J.; Papadakis, C. M.; Cubitt, R.; Müller-Buschbaum, P. *Macromolecules* **2009**, *42*, 9041.
- (20) Wang, W.; Kaune, G.; Perlich, J.; Papadakis, C. M.; Bivigou Koumba, A. M.; Laschewsky, A.; Schlage, K.; Röhlberger, R.; Roth, S. V.; Cubitt, R.; Müller-Buschbaum, P. *Macromolecules* **2010**, *43*, 2444.
- (21) Zhu, K.; Pamies, R.; Kjøniksen, A.-L.; Nyström, B. *Langmuir* **2008**, *24*, 14227.
- (22) Masci, G.; Giacomelli, L.; Crescenzi, V. *Macromol. Rapid Commun.* **2004**, *25*, 559.
- (23) Zhu, K.; Jin, H.; Kjøniksen, A.-L.; Nyström, B. *J. Phys. Chem. B* **2007**, *111*, 10862.
- (24) Beheshti, N.; Zhu, K.; Kjøniksen, A.-L.; Knudsen, K. D.; Nyström, B. *Soft Matter* **2011**, *7*, 1168.
- (25) Kjøniksen, A.-L.; Laukkanen, A.; Galant, C.; Knudsen, K. D.; Tenhu, H.; Nyström, B. *Macromolecules* **2005**, *38*, 948.
- (26) Kjøniksen, A.-L.; Zhu, K.; Pamies, R.; Nyström, B. *J. Phys. Chem. B* **2008**, *112*, 3294.
- (27) Siegert, A. J. F. *Radiation Laboratory Report No. 465*; Massachusetts Institute of Technology: Cambridge, MA, 1943.
- (28) Kjøniksen, A.-L.; Nyström, B.; Tenhu, H. *Colloids Surf., A* **2003**, *228*, 75.
- (29) Chen, H.; Ye, X.; Zhang, G.; Zhang, Q. *Polymer* **2006**, *47*, 8367.